TIME-DEPENDENT RAYLEIGH–BÉNARD CONVECTION AND INSTRUMENTAL ATTENUATION

R.P. BEHRINGER, C. AGOSTA, J.S. JAN and J.N. SHAUMEYER
Wesleyan University, Middletown, CT 06457, USA

We present new thermal data on time-dependent convection in a cylindrically confined layer of helium with aspect ratio $\Gamma = 7.87$ ($\Gamma \equiv$ layer radius/layer height). Experimental data and an analysis of attenuation effects indicate broadband spectral features obtained by a global probe tend to be independent of Γ for $\Gamma \gtrsim 5$.

When a layer of fluid is heated from below, Rayleigh–Bénard convection will occur if the temperature difference ΔT across the layer exceeds a critical value ΔT_c. Although much is understood [1] about the steady state flows which can be achieved for ΔT alightly above ΔT_c, the onset of time-dependent flow or turbulence has not yet yielded to a complete theoretical description. Accordingly, the onset of time-dependence has been the subject of a considerable number of recent experimental studies [2–11]. In this paper we present new thermal measurements for layers of normal liquid helium made in a cylindrical container of aspect ratio $\Gamma = 7.87$ ($\Gamma \equiv$ layer radius/layer height). In addition we consider an important effect which must be taken into account when analyzing thermal measurements, namely the effect of apparatus related attenuation. When this experimental effect is considered, the difference between measurements [5] of turbulence for $\Gamma = 57$ and for smaller Γ can be explained. The existing data including our new results indicate that the nature of steady broadband time-dependence tends to change very little with aspect ratio for $\Gamma \gtrsim 5$.

It is particularly convenient to express experimental results in terms of the reduced Rayleigh number R/R_c where the Rayleigh number R is

$$R \equiv g\alpha d^3 \Delta T / \kappa \nu; \tag{1}$$

g is the acceleration of gravity, d is the height of the fluid layer and the fluid parameters α, κ and ν are, respectively, the isobaric thermal expansion coefficient, the thermal diffusivity and the kinematic viscosity. When $\Delta T = \Delta T_c$, $R = R_c$. The remaining global properties specifying the state of the system are Γ and the Prandtl number σ with $\sigma = \nu/\kappa$. For our experiments $\sigma = 0.6$. A convenient time scale is $t_v = d^2/\kappa$, the vertical thermal diffusion time. For our experiment $d = 0.056$ cm, and $t_v = 4.7$ s or 7.8 s, depending on the mean temperature and pressure of the helium.

We maintain the top of the fluid layer at a fixed temperature and provide a constant heat flux to the bottom. We then observe time-dependence in the fluid by monitoring the fluctuations in the horizontally uniform temperature T_b at the bottom of the layer. This global technique is quite similar to that used by Ahlers [4] and by Ahlers and Behringer [5]. The appropriate boundary conditions differ slightly from the theoretically conventional ones because T_b is allowed to vary. However, the variations in T_b are quite small, no more than two percent of ΔT. The observed time-dependence is therefore intrinsic to the conventional problem. Our technique, however, provides considerably higher experimental resolution than measurements of the time-dependent heat flux needed to keep T_b fixed, an arrangement which would strictly meet the conventional assumptions.

We find that the convection is clearly time-dependent when $R/R_c \gtrsim 1.3$. This is consistent with the results of Libchaber and Maurer [7] as well as Ahlers and Behringer [5] who find clear time-dependence for $\Gamma \approx 5$ when $R/R_c \gtrsim 2.0$ and for $\Gamma = 57$ when R/R_c
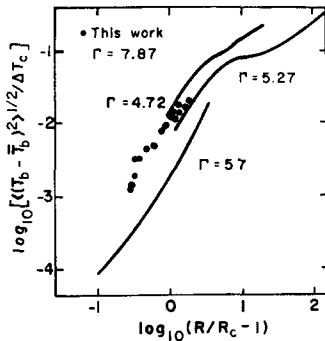
Fig. 1. The rms fluctuations $\langle\!\langle(T_b - \bar{T}_b)^2\rangle\rangle^{1/2}$ in the botton temperature T_b of the fluid container for several aspect ratios. The solid lines represent results presented in ref. [4] (Γ = 5.27) and ref. [5] (Γ = 4.72, Γ = 57). The results of this work are for Γ = 7.87.

$\gtrsim 1.0$. Our power spectra for T_b when $R/R_c \gtrsim 1.3$ are broadband with a single maximum at $\omega = 0$, where ω is the frequency. For small ω the power $P(\omega)$ is typically independent of the frequency, but then falls off for larger ω as ω^{-a} with $a = 4.0 \pm 0.2$. This type of spectrum was reported previously by Ahlers [4] and Ahlers and Behringer [5] for Γ = 5.27 and Γ = 4.72, respectively. Ahlers and Behringer also reported spectra for Γ = 57 which are somewhat different; these spectra, although broadband, show no frequency independent portion for low ω, and do not fall off as ω^{-4}, at least for the range of experimental frequencies.

In fig. 1 we show values for the rms fluctuations in T_b, $\langle\!\langle(T_b - \bar{T}_b)^2\rangle\rangle^{1/2}$, versus R/R_c for our results as well as those from previous experiments. These latter data are represented within their scatter by the appro-
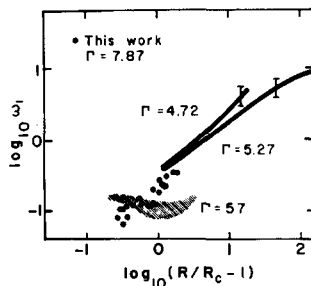

Fig. 2. The characteristic frequency $\omega_1 = (d^2/\kappa)[\int |\omega| \times P(\omega)\, d\omega]/[\int P(\omega)\, d\omega]$. The shaded regions and lines represent the data of ref. [4] (Γ = 5.27) and ref. [5] (Γ = 4.72, Γ = 57).

priately labeled lines. The rms values have been normalized by ΔT_c. In fig. 2 we show results for the characteristic frequency ω_1 defined by

$$\omega_1 = (d^2/\kappa)\left[\int |\omega| P(\omega)\, d\omega\right]\Big/\left[\int P(\omega)\, d\omega\right]. \quad (2)$$

The results for ω_1 and $\langle\!\langle(T_b - \bar{T}_b)^2\rangle\rangle^{1/2}$ with Γ = 4.78, 5.27 and 7.87 are strikingly similar. However, the results of ref. [5] for Γ = 57 tend to have lower values for ω_1 and $\langle\!\langle(T_b - \bar{T}_b)^2\rangle\rangle^{1/2}$. In the discussion below we point out a probable apparatus related cause for the difference between the data for Γ = 57 and those for Γ = 4.72, 5.27 and Γ = 7.87.

A typical experimental arrangement for thermal measurements is sketched in fig. 3. The fluid layer lies between two plates where the top plate is maintained at a fixed temperature. In one configuration the bottom plate is temperature-regulated at a higher temperature than the top plate by means of a heater and a thermometer, located a distance D from the fluid. Fluctuations in the temperature field of the convecting fluid layer lead to observable fluctuations in the amount of regulating heat supplied to the bottom plate. In a second configuration a constant amount of heat is supplied to the bottom of the fluid layer. The fluctuations in the temperature of the fluid layer result in fluctuations in the temperature recorded by the thermometer. This latter configuration was used in the present experiment and those of refs. [4,5].

The complete convection problem [1] involves the Navier–Stokes equations, the equation of continuity and the heat equation. For the present purposes only the last equation,

$$\partial T/\partial t + \mathbf{v} \cdot \boldsymbol{\nabla} T = \kappa \nabla^2 T, \quad (3)$$

is required. Here T is the temperature and $\mathbf{v}$ is the velocity of the fluid. The transfer of thermal signals from the fluid to the bottom plate involves only a
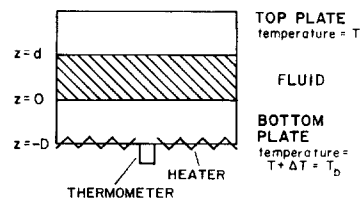

Fig. 3. Schematic of a typical experimental arrangement for thermal measurements of time-dependent convection.

very thin layer of the fluid near $z = 0$ as shown in fig. 3. In this region the velocity is quite small and may be set to zero. Usually, the bottom plate is a fairly good thermal conductor, and to a first approximation, T is independent of the horizontal directions, although for the purpose of these calculations it does depend on the vertical direction z. For the previous assumptions, the temporal Fourier transform of T, $\hat{T}(\omega, z)$ satisfies

$$-i\omega\hat{T} = \kappa \partial^2 \hat{T}/\partial z^2. \tag{4}$$

A similar equation applies inside the bottom plate except that κ must be replaced by κ_p, the thermal diffusivity for the plate. Inside the plate

$$\hat{T} = B_1 e^{iqz} + B_2 e^{-iqz}, \tag{5}$$

where

$$q = (1 + i)(\omega/2\kappa_p)^{1/2}. \tag{6}$$

At $z = 0$, T and $\lambda \partial T/\partial z$ are continuous assuming negligible boundary resistance. Here λ represents the appropriate thermal conductivity either for the fluid or for the plate, depending on whether $z > 0$ or $z < 0$. In the first experimental configuration above,

$$\hat{T}(\omega, -D) = 0, \tag{7}$$

for $\omega \neq 0$.

In the second experimental configuration

$$[\partial\hat{T}/\partial z]_{z=-D} = 0 \tag{8}$$

for $\omega \neq 0$. When eqs. (5), (6) and (8) are applied with the continuity conditions on $\hat{T}$ and $\lambda \partial \hat{T}/\partial z$, $\hat{T}(\omega, -D)$ is simply related to $\hat{T}(\omega, 0)$ by

$$\hat{T}(\omega, -D)/\hat{T}(\omega, 0) = 2/(e^{iqD} + e^{-iqD}). \tag{9}$$

Similarly, when eq. (8) is replaced by eq. (7), the ratio of the heat delivered at the bottom of the plate, to the heat fluctuations at the interface is

$$[\lambda\partial\hat{T}/\partial z]_{z=-D}/[\lambda\partial\hat{T}/\partial z]_{z=0} = 2/(e^{iqD} + e^{-iqD}). \tag{10}$$

Power spectra for the observed fluctuations in either T or $\partial T/\partial z$ differ from the true spectra by a factor of

$$H(\omega/\omega_0) = |2/(e^{iqD} + e^{-iqD})|^2 \tag{11}$$

$$= 2/[\cosh(\omega/\omega_0)^{1/2} + \cos(\omega/\omega_0)^{1/2}].$$
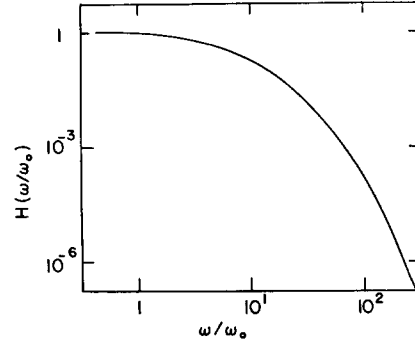

Fig. 4. The function $H(\omega/\omega_0) = 2/[\cosh(\omega/\omega_0)^{1/2} + \cos(\omega/\omega_0)^{1/2}]$ as a function of ω/ω_0.

Here,

$$\omega_0 = \kappa_p/2D^2. \tag{12}$$

Fig. 4 shows $H(\omega/\omega_0)$ versus ω/ω_0. As long as $\omega \lesssim \omega_0$, $H(\omega/\omega_0) \approx 1$ and the spectra are relatively unaffected. However, $H(\omega/\omega_0)$ falls off rapidly as ω/ω_0 increases above unity. A useful parameter is

$$Q \equiv \omega_0 d^2/\kappa = \tfrac{1}{2}(\kappa_p/\kappa)(d/D)^2. \tag{13}$$

When Q is large the fluctuation frequencies will tend to be small compared to ω_0 and $H \approx 1$. When Q is not large the observed spectra may differ considerably from their true form. Since $Q \propto (d/D)^2$, experiments done on very shallow layers or with thick bottom plates are particularly susceptible.

There are several instances in the literature for which the above damping effect should be considered. However, to our knowledge, the only data [5] for which Q is smaller than one is that obtained for an aspect ratio of $\Gamma = 57$. Each spectrum for $\Gamma = 57$ can be reasonably described by a constant times $H(\omega/\omega_0)$, with a single value of ω_0 consistent with the experimental arrangement. The similarity of the data to $H(\omega/\omega_0)$ suggests that over the range of observation, the true spectra are actually nearly flat, and that the asymptotic frequency dependence is not observed. Although the spectra are described rather well by $H(\omega/\omega_0)$, some caution must be taken in assuming complete agreement. The arrangement shown in fig. 3 is a condensation of the essential features, not an exact description of the experiment. However, the true attenuation function should be rather similar to $H(\omega/\omega_0)$.

On the basis of the previous discussion, the charac-

teristic frequencies ω_1 which were obtained for the Γ = 57 spectra may represent the damping effect of the container and not the true time-dependence of the fluid. In particular, values of ω_1 for Γ = 57 tend to be independent of R/R_c and lower than the corresponding results for aspect ratios of 4.72 and 7.87. In the latter cases container-related damping effects are probably not very serious. Of course, some caution must be taken in comparing the ω_1 data for Γ = 57 to that for smaller Γ, since in the former case, $2.94 \leqslant \sigma \leqslant 4.40$, while for the latter cases $0.6 \leqslant \sigma \leqslant 0.8$.

To conclude we have presented new data for time-dependent convection and we have examined an experimental problem which must be considered when interpreting thermal measurements of time-dependent convection. By means of fairly realistic assumptions it is possible to describe the attenuation of the thermal signal as it propagates from the fluid to the point of observation. The above description explains the differences between the spectra for Γ = 57 and the spectra for smaller aspect ratios such as Γ = 4.72, Γ = 5.27 and the new data for Γ = 7.87 which we have presented. The Rayleigh number for the onset of broadband time-dependence when $\sigma \approx 1$ clearly decreases with increasing Γ. However, the nature of broadband turbulence does not seem to change as Γ varies from 4.72 to 7.87, nor is there yet reason to assume that turbulence for

very large aspect ratios differs significantly from that for smaller aspect ratios with $\Gamma \gtrsim 5$.

References

[1] C. Normand, Y. Pomeau and M. Velarde, Rev. Mod. Phys. 49 (1977) 581, and references therein.
[2] J.P. Gollub and S.V. Benson, J. Fluid Mech. (1980).
[3] P. Berge and M. Dubois, Opt. Commun. 19 (1976) 129.
[4] G. Ahlers, Phys. Rev. Lett. 33 (1974) 1185, and in: Fluctuations, instabilities, and phase transitions, ed. T. Riste (Plenum, New York, 1975).
[5] G. Ahlers and R. Behringer, Phys. Rev. Lett. 40 (1978) 712; Prog. Theor. Phys., Suppl. 64 (1978) 186.
[6] H. Rossby, J. Fluid Mech. 36 (1969) 309.
[7] A. Libchaber and J. Maurer, J. de Phys. Lett. 39 (1978) L-369.
[8] G.E. Willis and J.W. Deardorff, Phys. Fluids 8 (1965) 2225; 10 (1967) 931; J. Fluid Mech. 44 (1970) 661.
[9] F.H. Busse and J.A. Whitehead, J. Fluid Mech. 66 (1974) 67.
[10] R. Krishnamurti, J. Fluid Mech. 42 (1970) 309.
[11] G. Ahlers and R.W. Walden, Phys. Rev. Lett. 44 (1980) 445.